Chapter

Design Optimization of 3D Steel Frameworks Under Constraints of Natural Frequencies of Vibration

Cláudio H.B. Resende, José P.G. Carvalho, Afonso C.C. Lemonge and Patricia H. Hallak

Abstract

Steel multistorey 3D frames are commonly used in business and residential buildings, industrial sheds, warehouses, etc. The design optimization of tall steel buildings is usually governed by horizontal loadings, such as, wind load, as well as its dynamic behavior, for which the structure must have the stiffness and stability in accordance with the safety criteria established by codes. This chapter deals with sizing structural optimization problems, concerning weight minimization of 3D steel frames, considering natural frequencies of vibration as well as allowable displacements as the constraints of the optimization problem. The discrete design variables are to be chosen from commercial profiles tables. A differential evolution (DE) is the search algorithm adopted coupled to an adaptive penalty method (APM) to handle the constraints. Three different 3D frames are optimized, presenting very interesting results.

Keywords: steel frame optimization, differential evolution, natural frequencies of vibration, wind load, adaptive penalty method

1. Introduction

Steel multistorey 3D frames are commonly used in business and residential buildings, industrial sheds, warehouses, etc. The design optimization of tall steel buildings is usually governed by horizontal loadings, such as, wind load, as well as its dynamic behavior, for which the structure must have the stiffness and stability following the safety criteria established by codes. The task of finding the most economical structures, that is, with the minimum weight and satisfying the constraints imposed by the codes, such as, ASD-AISC [1], NBR 6123 [2], and NBR 8800 [3], is not trivial. This may require an interactive process (trial and error) that may require very expensive or even impossible computational time. The behavior constraints include, for instance, combined bending and axial stress, shear stress, compression buckling, tension slenderness, drift ratio, multiple natural frequencies of vibration, elastic critical loads, etc.

This chapter is not an attempt to provide a survey of publications on structural optimization problems of multistorey 3D frames concerning many types of constraints. However, one can cite some papers where readers can find reviews regarding this issue.

An optimization process via genetic algorithms using MATLAB-SAP2000 Open Application Programming Interface (OAPI) is presented for optimum design of space frames with semirigid connections in Artar and Daloğlu [4].

An enhanced imperialist competitive algorithm for optimum design of skeletal structures is proposed by Maheri and Talezadeh [5]. In Aydoğdu et al. [6], an enhanced artificial bee colony algorithm is adopted to find the optimum design problem of steel space frames formulated according to the provisions of LRFD-AISC. Talatahari et al. [7] proposed the combination of an eagle strategy algorithm with the differential evolution (DE) which is implemented by interfacing SAP2000 structural analysis code and MATLAB mathematical software to find the optimum design of framed structures. Maheri et al. [8] proposed an enhanced honey bee mating optimization algorithm for the design of side sway steel frames. The robustness of the algorithm in terms of both solution quality and computational cost is proven by solving four design optimization problems of side sway steel frames. Optimal seismic design of three-dimensional steel frames is carried out in Kaveh and BolandGerami [9] with the structures subjected to gravity and earthquake loadings and designed according to the LRFD-AISC design criteria.

The harmony search metaheuristic is used as the search engine. Kaveh and BolandGerami [9] used a cascade-enhanced colliding body optimization to find the optimum design of large-scale space steel frames according to ASD-AISC. Jalili et al. [10] presented a modified biogeography-based optimization (MBBO) algorithm for the optimum design of skeletal structures with discrete variables. Gholizadeh and Poorhoseini [11] proposed a modified dolphin echolocation (MDE) algorithm proposed for the optimization of steel frame structures. Gholizadeh and Milany [12] used an improved fireworks algorithm (IFWA) to deal with the discrete structural optimization problems of steel trusses and frames.

Since the tall buildings present the need for in-depth analyses regarding their lateral stability, several studies are found in the literature on this subject. Cost efficiencies of various steel frameworks are investigated for the economical design of multistorey buildings by Hasançebi [13]. Braced and unbraced steel frames subjected to gravity and lateral seismic loads were studied by Memari and Madhkan [14]. Kameshki and Saka [15] compared pin-jointed frames considering several types of bracings with rigidly connected frames without bracings. Liang et al. [16] applied a performance-based design optimization method to discover optimum topologies of bracings for steel frames. In his paper Hasançebi [13] highlights important aspects regarding restrictions on the fabrication of structural elements. In this sense, it is essential. In this sense, it is imperative that construction costs of the resulting structures, rather than design weights only, must be evaluated. Studies on this subject were conducted by Pavlovčič et al. [17].

This chapter deals with sizing structural optimization problems, concerning weight minimization of 3D steel frames, considering natural frequencies of vibration as well as allowable displacements as the constraints of the optimization problem. The discrete design variables are to be chosen from commercial profile tables. A DE [18] is the search algorithm adopted coupled with an adaptive penalty method (APM) to handle the constraints [19]. An essential aspect of this chapter is the importance that must be given concerning the constraints regarding the first natural frequency of vibration of the frames. Often, they are neglected in the formulations of these structural optimization problems. A brief review of optimization problems considering natural frequencies of vibration as constraints is provided by Carvalho et al. in [20].

This chapter is as organized as follows: Section 2 presents the formulation of the optimization problem. Section 3 presents the basics concepts on differential evolution algorithm and the strategy to handle the constraints. Numerical experiments and analysis of results are described in Sections 4 and 5, respectively. Finally, the conclusions and extensions of this chapter are described in Section 6.

2. Formulation of the optimization problem

The optimization problem deals with the weight minimization of 3D steel frames consisting of N members, under constraint of natural frequencies of vibration and allowable displacements due to design loads.

The objective is to find an integer index vector $\mathbf{x}$ (Eq. (1)) which points to commercial steel profile where each index i points to a cross-sectional area (A_i), the inertias about the main axes (I_{xi}, I_{yi}) and the torsional constant (I_{ti}). These properties are used to define a candidate solution in the evolutionary process. Two different search spaces are adopted for columns and beams, containing 29 and 56 available profiles, respectively, provided in **Table 1**.

$$\mathbf{x} = \{I_1, I_2, \ldots, I_i\} \tag{1}$$

The objective function $w(\mathbf{x})$ (Eq. (2)) is the weight of the structure, in which L_i is the length, A_i is the cross-sectional area, and ρ_i *is* the specific mass of the ith member. 7850 kg/m^3 is the specific mass of the steel used in the numerical experiments presented in this chapter.

$$w(\mathbf{x}) = \sum_{i=1}^{N} \rho_i A_i L_i \tag{2}$$

The maximum horizontal displacement and the first natural frequency of vibration are the constraints written as

	Case 1			Case 2		
dv	**[19]**	**[21]**	**TS**	**[22]**	**[20]**	**TS**
A_1	29.2257	30.520	30.268	5.5713	5.4870	5.6593
A_2	0.1000	0.100	0.1018	2.4072	2.2475	2.2830
A_3	24.1821	23.200	23.1493	5.4692	5.5000	5.3987
A_4	14.9471	15.220	15.2456	2.3847	2.2320	2.3229
A_5	0.1000	0.100	0.1001	0.1004	0.1000	0.1000
A_6	0.3946	0.551	0.5546	0.7104	0.7285	0.7159
A_7	7.4958	7.457	7.4902	3.6596	3.7976	3.6969
A_8	21.9249	21.040	21.3433	3.6579	3.7820	3.7667
A_9	21.2909	21.530	21.3958	2.0703	1.9840	1.9386
A_{10}	0.1000	0.100	0.1001	1.9153	1.9065	1.9351
W	5069.09	5060.80	5061.45	532.390	532.124	532.03
nfe	28,0000	—	10,000	21,000	21,000	10,000

Table 1.
Comparison of results of the 10-bar truss.

$$\frac{\delta_{\max}(\mathbf{x})}{\bar{\delta}} - 1 \le 0$$
$$1 - \frac{f_1(\mathbf{x})}{\bar{f}_1} \le 0 \tag{3}$$

where δ_{max} is the maximum displacement at the top of the structure, $\bar{\delta}$ is the maximum allowable displacement, f_1 is the first natural frequency of vibration, and $\bar{f}_1$ is the minimum allowed frequency by the standard codes.

3. Differential evolution algorithm and the adaptive penalty scheme

The algorithm used in this study is the traditional DE algorithm, which was introduced in 1995 by Storn and Price [18]. It is based on evolution of population of vectors in the search space. This algorithm has been showing robustness in solving structural mono- and multi-objective optimization problems.

The first step of the algorithm consists of generating a pseudorandom population in the search space. Then, the evolution of the vectors is governed by Eq. (4):

$$\mathbf{x}_{j,i,G} \leftarrow \mathbf{x}_{j,r1,G} + \boldsymbol{F}\left(\mathbf{x}_{j,r2,G} - \mathbf{x}_{j,r3,G}\right) \tag{4}$$

where $\boldsymbol{x}_{j,i,G}$ represents the new individual of the new generation; $\boldsymbol{x}_{j,r1,G}$, $\boldsymbol{x}_{j,r2,G}$, and $\boldsymbol{x}_{j,r3,G}$ represent, respectively, the base vector and two other vectors from the previous generation (both three vectors are randomly selected and different among them); and F represents the scale factor of the difference between vectors. This expression (Eq. 4) is illustrated in **Figure 1**.

Mutation and crossover operators are considered in the differential evolution, and there is a predetermined probability of crossover (Pcr) as well as a probability of mutation between the new and the old individual.

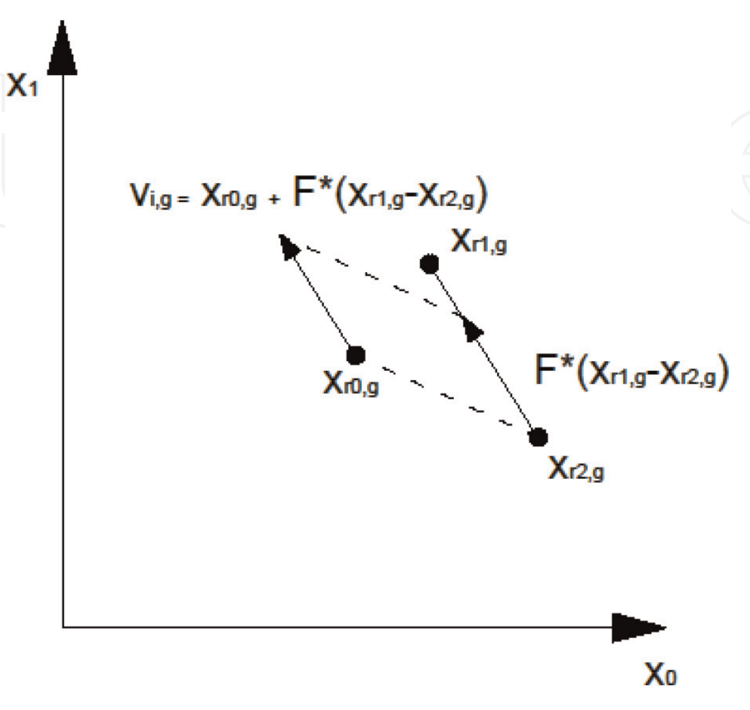

Figure 1.
Visual representation of DE scheme.

The following flowchart represents the scheme of DE:

Initialize pseudorandom population
For i = 1: NPOP
    Select randomly J ∈ {1,…, NPOP}
    For j = 1: NPOP
        Select randomly *rand* ∈ [0, 1]
        If rand < Pcr or j = J
            $\mathbf{x}_{j,i,G} \leftarrow \mathbf{x}_{j,r1,G} + \boldsymbol{F}\left(\mathbf{x}_{j,r2,G} - \mathbf{x}_{j,r3,G}\right)$
        Else
            $\mathbf{x}_{j,i,G} \leftarrow \mathbf{x}_{j,r1,G}$
        end if
    end For
end For

where NPOP represents the number of population.

To handle the constraints, the APM is adopted, proposed by Lemonge and Barbosa [19].

The fitness function $W(\mathbf{x})$ is defined by Eq. (5).

$$W(\mathbf{x}) = \begin{cases} w(\mathbf{x}), & \text{if } \mathbf{x} \text{ is feasible} \\ \overline{w}(\mathbf{x}) + \sum\limits_{jj=1}^{n_c} k_{jj} v_{jj}(\mathbf{x}), & \text{otherwise} \end{cases} \tag{5}$$

where $w(\boldsymbol{x})$ is the objective function of the candidate solution without penalization Eq.(6)

$$\overline{w}(\mathbf{x}) = \begin{cases} w(\mathbf{x}), & \text{if } w(\mathbf{x}) > \langle w(\mathbf{x}) \rangle \\ \langle w(\mathbf{x}) \rangle, & \text{if } w(\mathbf{x}) \le \langle w(\mathbf{x}) \rangle \end{cases} \tag{6}$$

where $\langle w(\boldsymbol{x}) \rangle$ is the average value of the objective function of the solutions of the current population. The penalty parameter k_{jj} is defined in Eq.(7):

$$k_{jj} = |\langle w(\mathbf{x}) \rangle| \frac{\langle v_{jj}(\mathbf{x}) \rangle}{\sum_{ll=1}^{n_c} [v_{ll}(\mathbf{x})]^2}, \tag{7}$$

where $\langle v_{jj}(\mathbf{x}) \rangle$ means the violation of the jj-th constraint averaged over the current population considering only infeasible individuals. The complete formulation of the APM can be found in [19].

4. Numerical examples

4.1 Preliminary experiment

To validate the proposed search mechanism, a well-known benchmark 10-bar truss, shown in **Figure 2**, is considered. Two cases are analyzed: in the first one, the problem consists of weight minimization considering displacements and stresses as constraints and, in the second case, minimization of its weight considering natural frequencies as constraints; for both cases the design variables are the cross-sectional areas of the bars (totalizing 10 variables). The truss has Young's modulus equal to

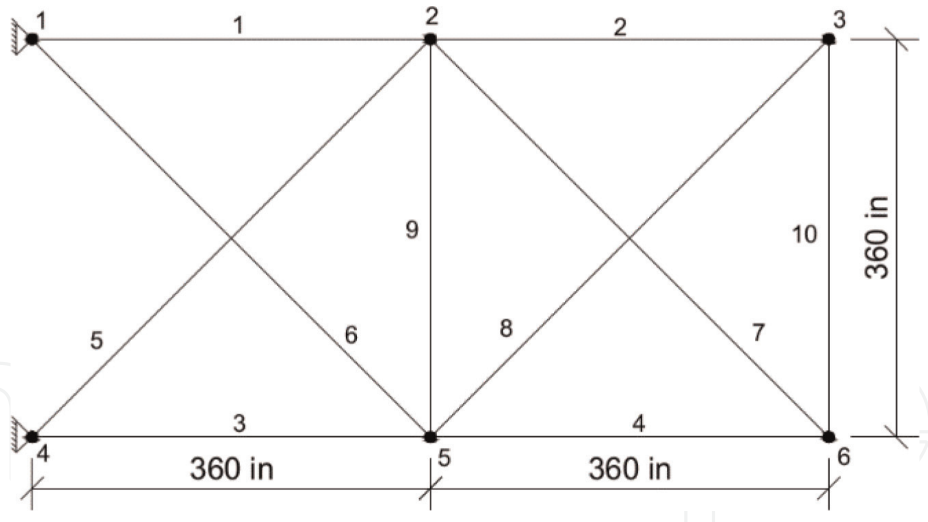

Figure 2.
The 10-bar truss.

10^4 ksi (68.95 GPa) and material density equal to 0.1 lb/in³ (2770 kg/m³). For case 1, the upper and lower bounds are equal to 0.1 and 33.50 in^2, and two loads of 100 kips (444.82 kN) each are applied at nodes 2 and 4; for case 2, the bounds are equal to 0.1 and 7.75 in^2, and an additional mass of 1000 lbs. (454.54 kg) is attached to free nodes (1–4). Constraints are set to ±25 ksi (for both compression and tension) and 2 inches for case 1, and also $f_1 \geq 7$ Hz, $f_2 \geq 15$ Hz, and $f_3 \geq 20$ Hz for case 2.

Table 2 shows the design variables (*dv*) (in^2 for case 1 and cm^2 for case 2), the optimum weights (*W*) (lb for case 1 and kg for case 2) obtained for both cases, as well as a comparison with some results found in the literature where TS means the results obtained with this study. For both cases, 50 independent runs were performed; the population size is 50 which evolved in 200 generations leading to 10,000 function evaluations (*nfe*).

4.2 Design loads

The first mutlistorey 3D steel frame is a simple three-storey steel frame, with 3 m of width, 6 m of length, and 9 m of height equally spaced. This 3D frame is subjected to lateral wind and gravity loads. The gravity and wind loads are defined based on the Brazilian technical codes NBR 6123 [2], detailed on the next subsections. The model in finite elements for the first 3D frame consists in 39 members and 24 joints depicted in **Figure 3**.

4.2.1 Wind loads

To define the forces due to the wind on the columns, it demands to determine the dynamic pressure (q) acting on the area of the larger façade. For this purpose, two parameters, the wind basic velocity (V_0) and the wind characteristic velocity (V_k), are necessary. The basic velocity V_0 is inherent of the region and assumed as the velocity of 3 s gust, exceeded in mean once in 50 years, 10 m above the ground on an open and plain field. For the city of Juiz de Fora, Minas Gerais State, Brazil, the basic velocity is equal to V_0 = 35 m/s. The characteristic velocity is defined by Eq. (8), where S_1 (topographic factor), S_2(terrain roughness factor), and S_3(statistic factor) are weighting coefficients resulting in 25.9 m/s as written in Eq. (9) ([2]).

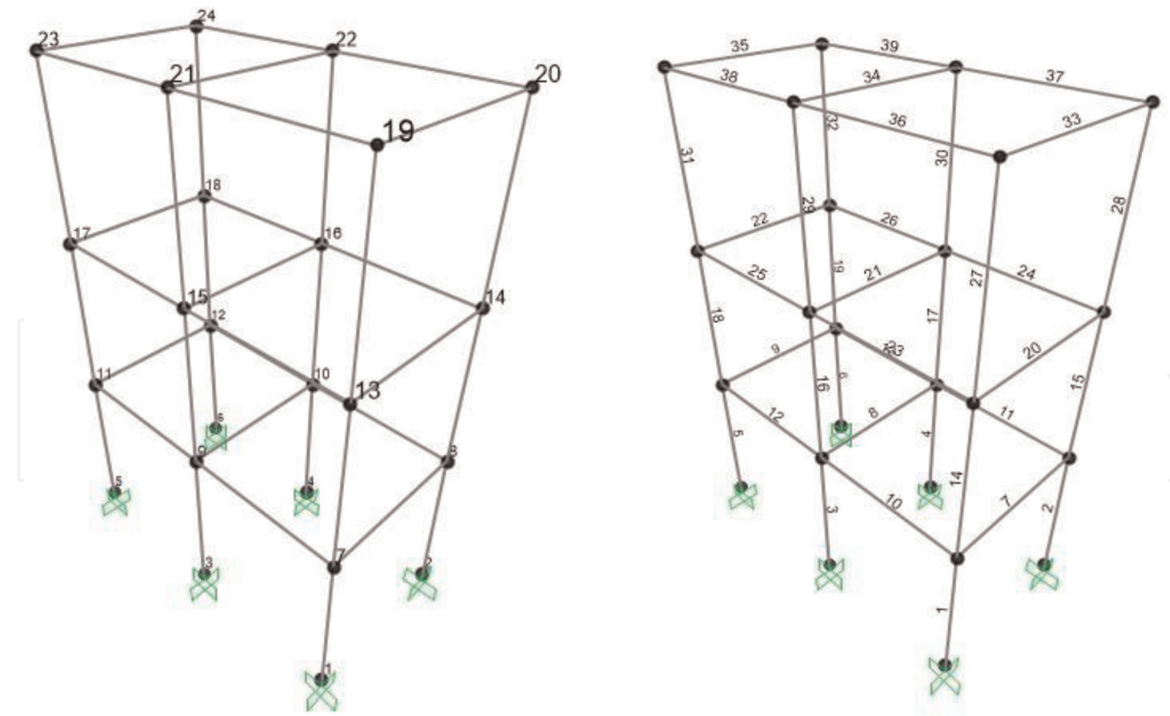

Figure 3.
The 39 members frame—joints and elements mapping.

$$V_k = V_0 S_1 S_2 S_3 \tag{8}$$

$$V_k = 35 \times 1.0 \times 0.74 \times 1.0 = 25.9 \text{ m/s} \tag{9}$$

With the characteristic velocity, it is possible to determine the dynamic pressure on the larger facade of the frame through Eq. (10).

$$q = 0.613 V_k^2 = 0.613 \times 25.9^2 = 411.21 \text{ N/m}^2 \tag{10}$$

The dynamic pressure acting on the frame's larger facade, q = 0.411 kN/m^2, must be transferred as a uniform load applied to the columns; to transfer the area loading to columns, the influence area of corner columns (CC) (red area = 13.5 m^2) and middle columns (MC) (blue area 27 m^2) are used; the steps are detailed in Eqs.(11) and (12) and **Figure 4**, where P_c and P_M are the uniform wind load on the corner columns and middle columns, respectively.

$$P_C = 0.411 \frac{\text{kN}}{\text{m}^2} \times \frac{13.5 \text{ m}^2}{9 \text{ m}} = 0.62 \text{ kN/m} \tag{11}$$

$$P_M = 0.411 \frac{\text{kN}}{\text{m}^2} \times \frac{27 \text{ m}^2}{9 \text{ m}} = 1.23 \text{ kN/m} \tag{12}$$

4.2.2 Gravity loads

Two different types of gravity loads are considered: dead loads and live loads. The first one refers to self-weight of the structural elements, such as, the concrete slabs, which was adopted with a thickness equal to 10 cm, and the second one corresponds to the occupation. The dead load acting on the floor is 3 kN/m^2, and the live is 2 kN/m^2. The inner beams (IB) would be more loaded (the largest influence area) than the outer beams (OB), as can be observed in **Figure 5**. The blue area (4.5 m^2) transfers its weight to the inner beams, and the red area (2.25 m^2) transfers

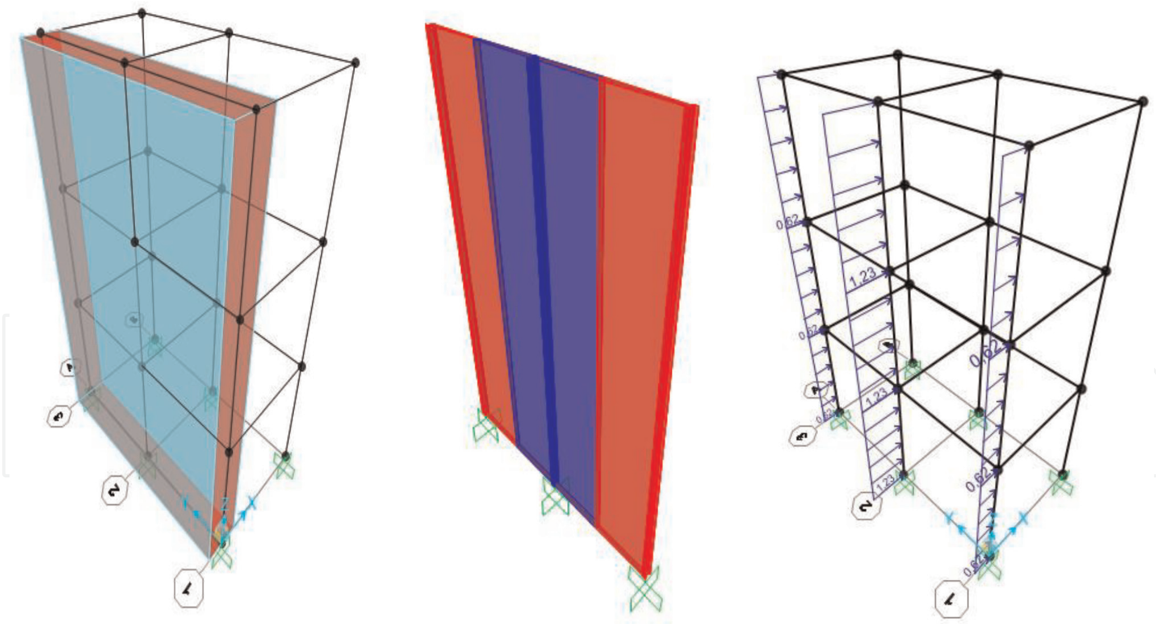

Figure 4.
Wind loads on columns.

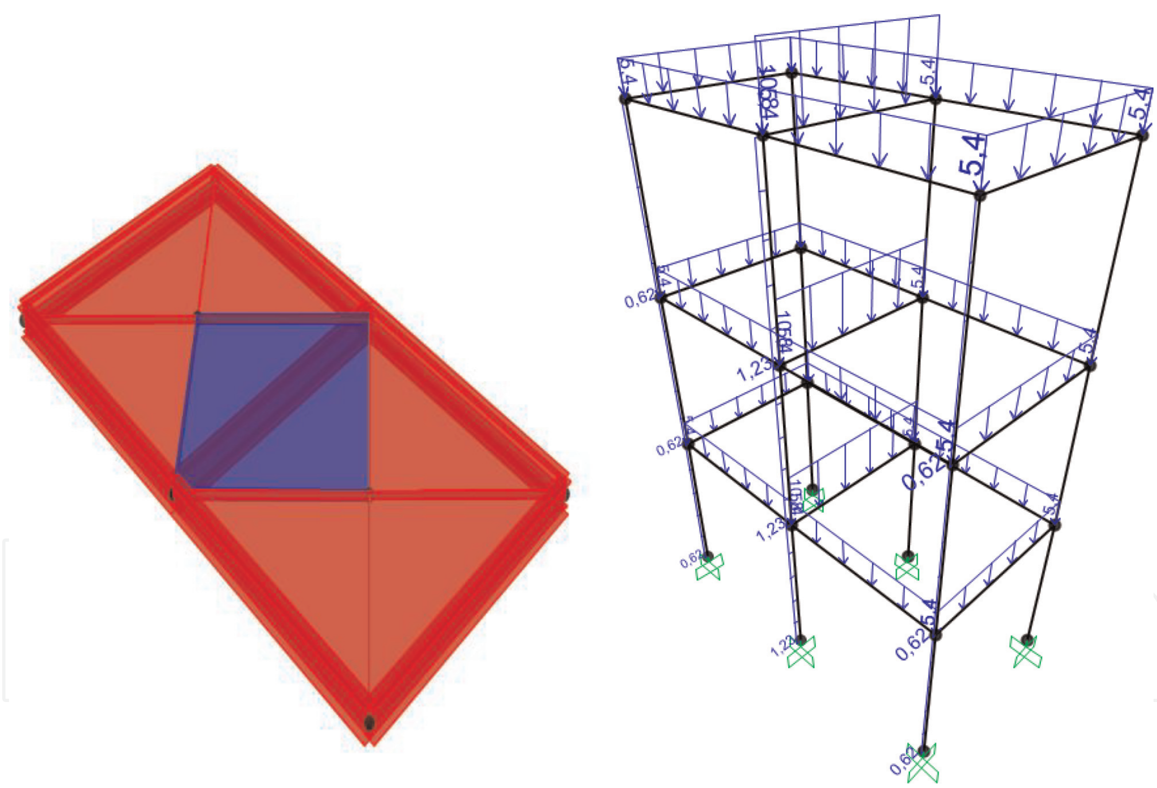

Figure 5.
Influence area for beams—design loads.

its weight to the outer beams. The design factor used for dead loads was 1.4 and for the live loads 1.5, according to the Brazilian Technical Standard code [2]. Eqs. (13) and (14) summarize the calculus of the design loads adopted in the experiments, according to the Brazilian Technical Standard code, where P_i and P_o are the uniform loading on inner beams and outer beams, respectively [3].

$$P_i = \left(1.4 \times 3\frac{\text{kN}}{\text{m}^2} + 1.5 \times 2\frac{\text{kN}}{\text{m}^2}\right) \times \frac{4.5\ \text{m}^2}{3\ \text{m}} = 10.8\ \text{kN/m} \qquad (13)$$

Profiles for columns		Profiles for beams			
W 150 × 22.5	W 250 × 89	W 150 × 13	W 310 × 21	W 410 × 38.8	W 530 × 66
W 150 × 29.8	W 250 × 101	W 150 × 18	W 310 × 23.8	W 410 × 46.1	W 530 × 72
W 150 × 37.1	W 250 × 115	W 150 × 24	W 310 × 28.3	W 410 × 53	W 530 × 74
W 200 × 35.9	W 310 × 79	W 200 × 15	W 310 × 32.7	W 410 × 60	W 530 × 82
W 200 × 41.7	W 310 × 93	W 200 × 19.3	W 310 × 38.7	W 410 × 67	W 530 × 85
W 200 × 46.1	W 310 × 97	W 200 × 22.5	W 310 × 44.5	W 410 × 75	W 530 × 92
W 200 × 52	W 310 × 107	W 200 × 26.6	W 310 × 52	W 410 × 85	W 530 × 101
W 200 × 53	W 310 × 110	W 200 × 31.3	W 360 × 32.9	W 460 × 52	W 530 × 109
W 200 × 59	W 310 × 117	W 250 × 17.9	W 360 × 39	W 460 × 60	W 610 × 101
W 200 × 71	W 310 × 125	W 250 × 22.3	W 360 × 44	W 460 × 68	W 610 × 113
W 200 × 86	W 360 × 91	W 250 × 25.3	W 360 × 51	W 460 × 74	W 610 × 125
W 250 × 62	W 360 × 101	W 250 × 28.4	W 360 × 57.8	W 460 × 82	—
W 250 × 73	W 360 × 110	W 250 × 32.7	W 360 × 64	W 460 × 89	—
W 250 × 80	W 360 × 122	W 250 × 38.5	W 360 × 72	W 460 × 97	—
W 250 × 85	—	W 250 × 44.8	W 360 × 79	W 460 × 106	—

Table 2.
Discrete search spaces for columns and beams.

$$P_o = \left(1.4 \times 3\frac{\text{kN}}{\text{m}^2} + 1.5 \times 2\frac{\text{kN}}{\text{m}^2}\right) \times \frac{2.25\ \text{m}^2}{3\ \text{m}} = 5.4\ \text{kN/m} \tag{14}$$

4.3 Experiment 1

The first experiment consists of the three-storey steel frame to minimize the weight as depicted in **Figure 3**, considering the loads discussed in the previous subsection subjected to the maximum horizontal displacements as the constraint that occur on the top of the frame. The frame has 9 m of height leading to an allowable displacement at the top equal to 22.5 mm as Eq. (15) shows:

$$\bar{\delta} = \frac{H}{400} = \frac{9000}{400} = 22.5\ \text{mm} \tag{15}$$

Five independent runs and 100 generations with a population of 50 individuals are the parameters set for DE. The best solution found is detailed in **Figure 5**. It is possible to note that the algorithm reached both the lightest profile for beams and columns, which are W 150 × 13 (red) and W 150 × 22.5 (blue), respectively, leading to a final weight of 2050 kg. For the best solution found, rigorously feasible in the evolutionary process, the maximum displacement is 19.6 mm as can be observed in the scale of **Figure 6**.

4.4 Experiment 2

The second experiment has the same characteristics as the first one. However, a constraint concerning the first natural frequency of vibration is added (Eq. (16)) that must be at least 4 Hz, according to the dynamic comfort values prescribed by NBR 8800 [3]. The natural frequencies are obtained calculating the eigenvalues of the matrix $[(f_{nf}^2 \text{ x M + K})]$ [23], where M and K are the mass and stiffness matrices,

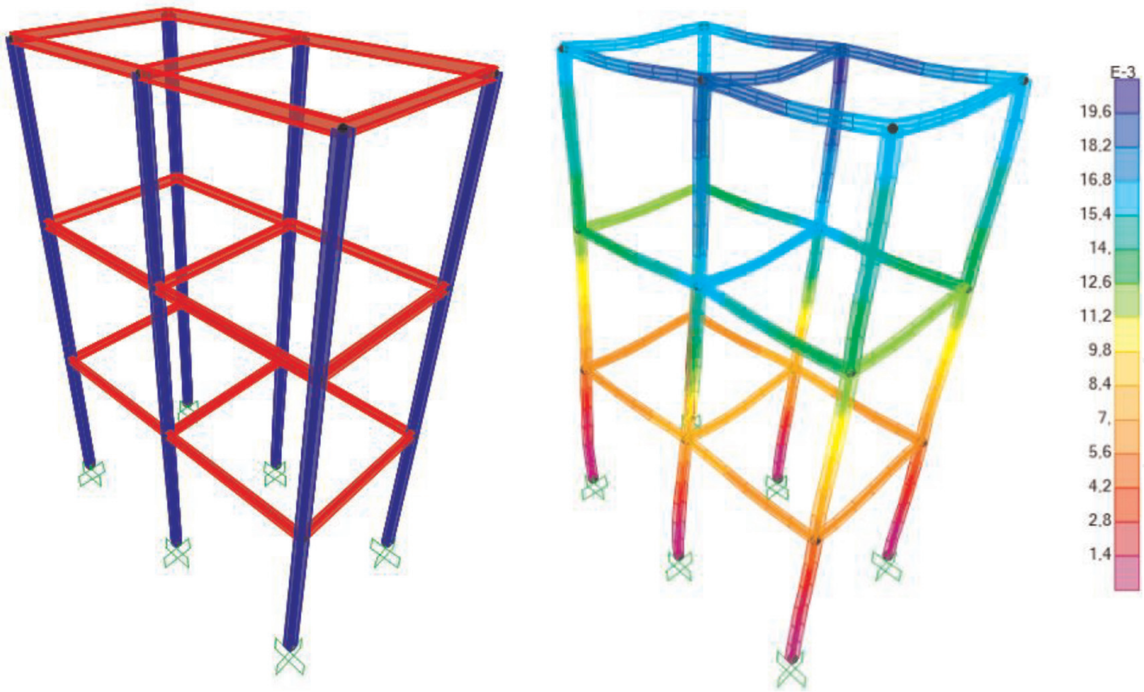

Figure 6.
The best solution and the displacement field for the Experiment 1.

respectively, and f_{nf} is the equivalent eigenvectors concerning the nf natural frequencies of vibration of the structure. Also a member grouping is adopted, considering the symmetry of structure. In optimized structures, it can be attractive to use a reduced number of distinct cross-sectional areas to minimize the costs of fabrication, transportation, storing, checking, and welding, thereby providing labor savings.

Thus, the member grouping is conducted such as corner columns, middle columns, outer beams, and inner beams (IB) form four different groups which each group will have the same profile as defined in **Figure 7** and **Table 3**.

$$\begin{aligned} &\frac{\delta_{\max}(\mathbf{x})}{22.5} - 1 \leq 0 \\ &1 - \frac{f_1(\mathbf{x})}{4} \leq 0 \end{aligned} \tag{16}$$

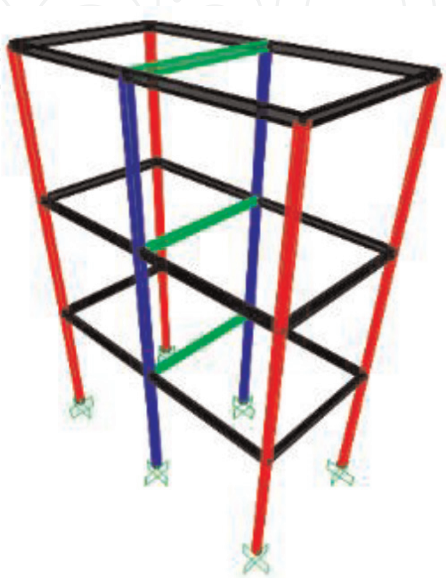

Figure 7.
Member grouping for the Experiment 2.

Group	Characteristics	Color
1	Corner columns	Red
2	Middle columns	Blue
3	Inner beams	Green
4	Outer beams	Black

Table 3.
Member grouping for the Experiment 2.

The DE parameters are the same in Experiment 1. The best solution found presented a final weight of 2587 kg, the maximum displacement of 12.9 mm, and the first natural frequency of vibration equal to 4.14 Hz corresponding, as expected, to a feasible solution. It is interesting to note that the algorithm distributed masses along the structure in a better way in order to satisfy the frequency constraint, in this case, decreasing the maximum displacement. **Figure 8** and **Table 4** show the detailed results.

4.5 Experiment 3

This numerical experiment consists in to minimize the weight of a 3D steel frame with six-storeys and 78 members, as illustrated in **Figure 9**, and it is subjected to wind load and a constraint concerning the maximum horizontal displacement at the top of the frame. In this experiment, distinct member groupings are adopted to show how the final weights decrease as more different profiles are used. In this sense, the members are grouped in two, four, and eight groups independently.

The wind and gravity loads are defined in the same way as the previous experiment, and the displacement constraint is written as (Eq. (17)):

$$\bar{\delta} = \frac{H}{400} = \frac{18000}{400} = 45 \text{ mm} \tag{17}$$

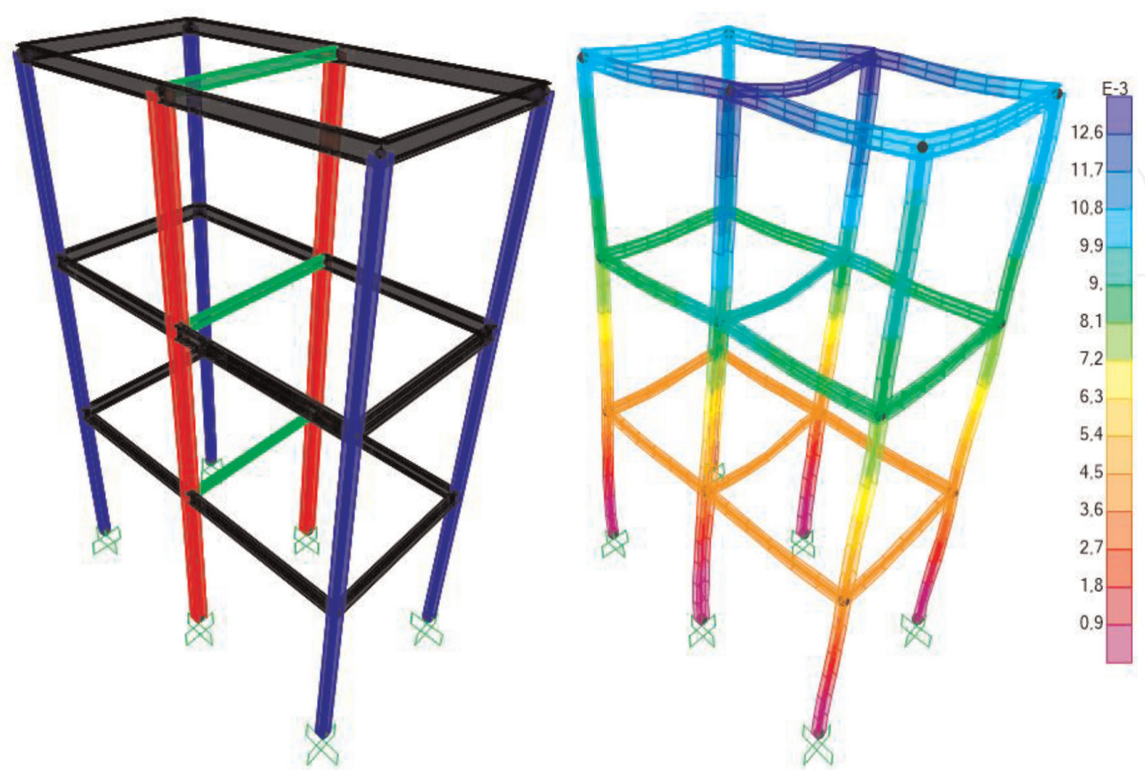

Figure 8.
The best solution and the displacement field for the Experiment 2.

Group	Characteristics	Color	Cross section
1	Corner columns	Red	W 150 × 22.5
2	Middle columns	Blue	W 200 × 46.1
3	Inner beams	Green	W 150 × 13
4	Outer beams	Black	W 200 × 15
Maximum displacement		—	12.9 mm
First natural frequency		—	4.14 Hz
Total weight		—	2587 kg

Table 4.
Optimum solution found for the Experiment 2.

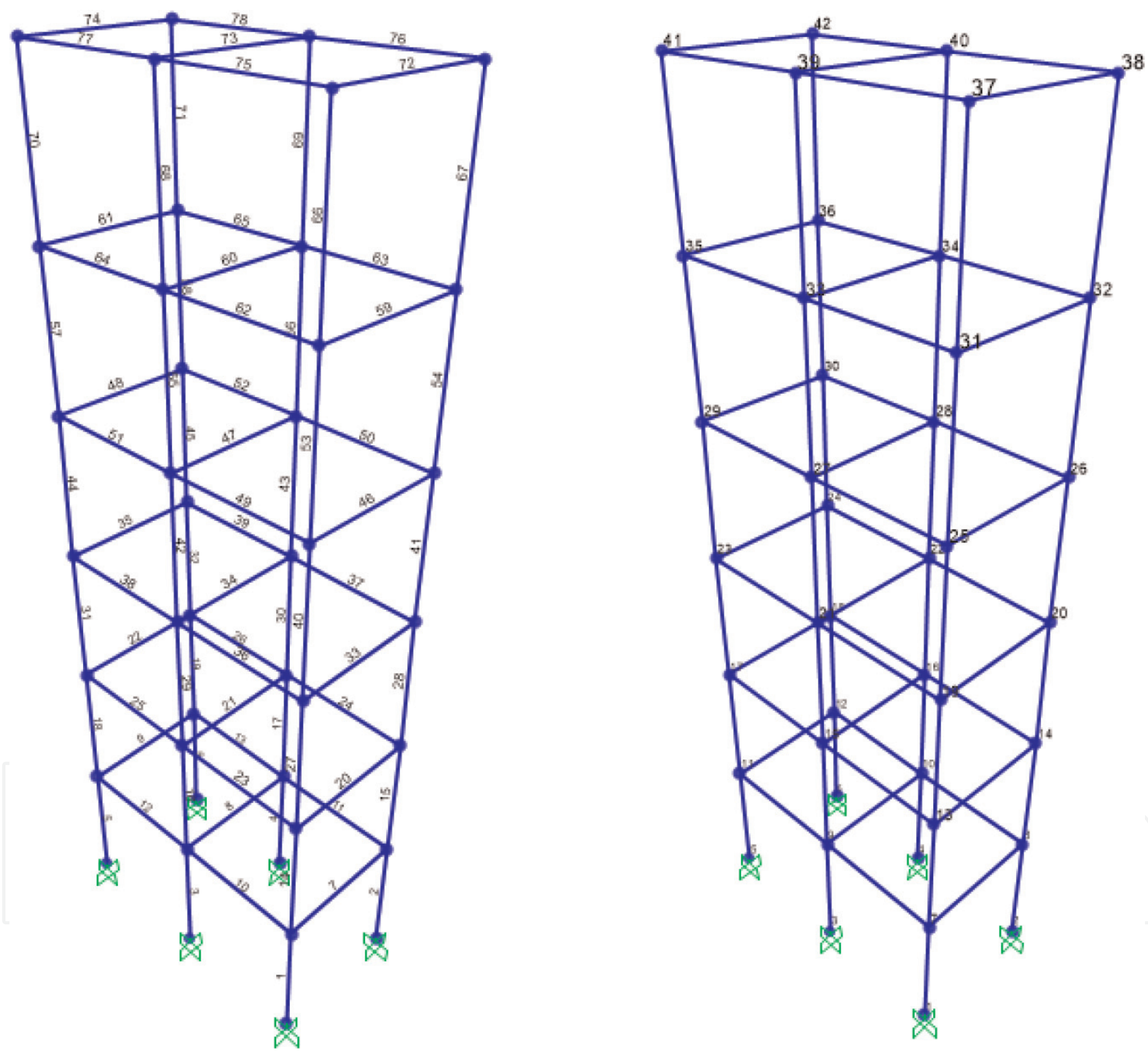

Figure 9.
The 78 members frame joints and elements mapping.

4.5.1 Members linked in two groups

Firstly, the problem considers the possibility of using only two distinct profiles, one for the columns and other for the beams. The member grouping adopted is described in the **Table 5** and in **Figure 10**.

The DE parameters are the same as Experiment 2, and best solution found is detailed in **Table 6** and in **Figure 11**.

Group	Characteristics	Color
1	Columns	Red
2	Beams	Blue

Table 5.
Experiment 3.1—members linked in two groups.

Figure 10.
Experiment 3.1—members linked in two groups according to ***Table 5****.*

Group	Characteristics	Color	Cross section
1	Columns	Red	W 150 × 29.8
2	Beams	Blue	W 360 × 44
Maximum displacement			22.6 mm
Total weight			8971 kg

Table 6.
The best solution of Experiment 3.1.

4.5.2 Members linked in four groups

In the second analysis of Experiment 3, the members are linked in four distinct groups as described in **Table 7** and **Figure 12**, and the best result found is detailed in **Figure 13** and **Table 8**.

4.5.3 Members linked in eight groups

Finally, the same problem is optimized with the members linked in eight groups as shown in **Table 9** and **Figure 14**. **Table 10** and **Figure 15** show the best solution found for Experiment 3.3.

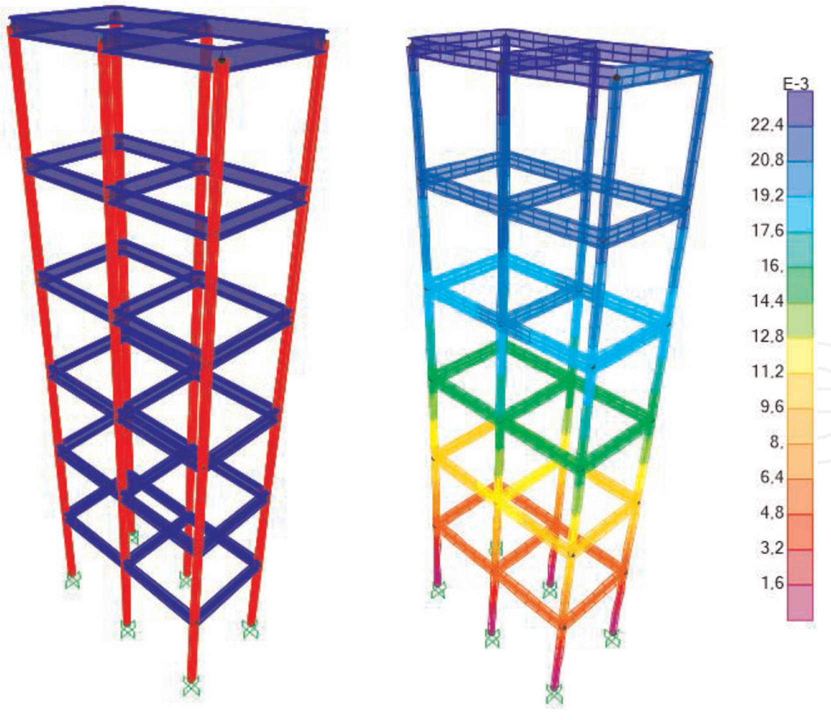

Figure 11.
The best solution and displacement field of Experiment 3.1.

Group	Characteristics	Color
1	Corner columns	Red
2	Middle columns	Black
3	Inner beams	Green
4	Outer beams	Blue

Table 7.
Experiment 3.2—members linked in four groups.

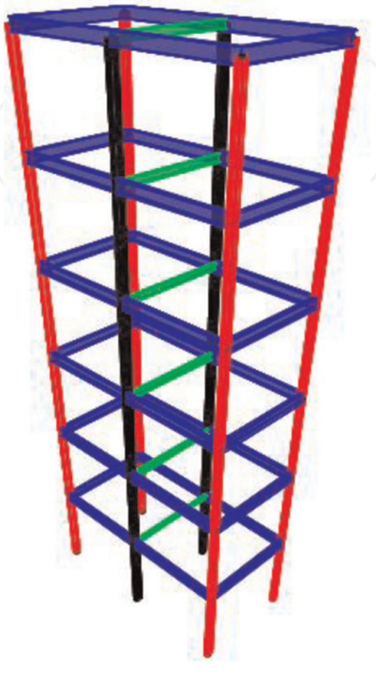

Figure 12.
Experiment 3.2–members linked in four groups according to ***Table 7****.*

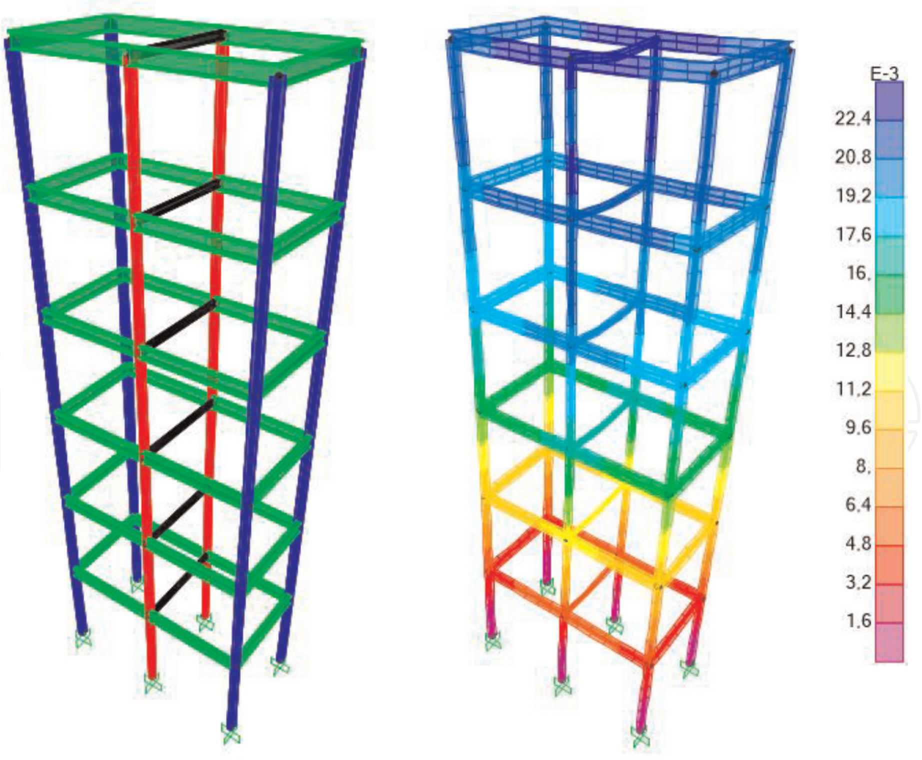

Figure 13.
The best solution and displacement field of Experiment 3.2.

Group	Characteristics	Color	Cross section
1	Corner columns	Blue	W 200 × 35.9
2	Middle columns	Red	W 150 × 22.5
3	Inner beams	Black	W 150 × 13
4	Outer beams	Green	W 310 × 38.7
Maximum displacement			23 mm
Total weight			7851 kg

Table 8.
The best solution of Experiment 3.2.

Group	Characteristics	Color
1	Corner columns—floors 1, 2, and 3	Blue
2	Middle columns—floors 1, 2, and 3	Red
3	Inner beams—floors 1, 2, and 3	Green
4	Outer beams—floors 1, 2, and 3	Black
5	Corner columns—floors 4, 5, and 6	Cyan
6	Middle columns—floors 4, 5, and 6	Magenta
7	Inner beams—floors 4, 5, and 6	Yellow
8	Outer beams—floors 4, 5, and 6	Gray

Table 9.
Experiment 3.3—members linked in eight groups.

Figure 14.
Experiment 3.3—members linked in eight groups according to **Table 9**.

Group	Characteristics	Color	Cross section
1	Corner columns—floors 1, 2, and 3	Blue	W 200 × 46.1
2	Middle columns—floors 1, 2, and 3	Cyan	W 150 × 22.5
3	Inner beams—floors 1, 2, and 3	Red	W 150 × 13
4	Outer beams—floors 1, 2, and 3	Black	W 310 × 38.7
5	Corner columns—floors 4, 5, and 6	Cyan	W 150 × 22.5
6	Middle columns—floors 4, 5, and 6	Cyan	W 150 × 22.5
7	Inner beams—floors 4, 5, and 6	Red	W 150 × 13
8	Outer beams—floors 4, 5, and 6	Gray	W 250 × 32.7
Maximum displacement			26 mm
Total weight			7421 kg

Table 10.
The best solution of Experiment 3.3.

4.6 Experiment 4

This experiment considers the first natural frequency of vibration as an additional constraint (Eq. (18)) to the six-storey 3D frame. However, the DE did not find any feasible solution. Thus, a new frame presenting 114 members (**Figure 16**) with bracings is proposed to stiffen the candidate solutions, rising the chances of reaching feasible solutions.

DOI: http://dx.doi.org/10.5772/intechopen.87022

Figure 15.
The best solution and displacement field of Experiment 3.3.

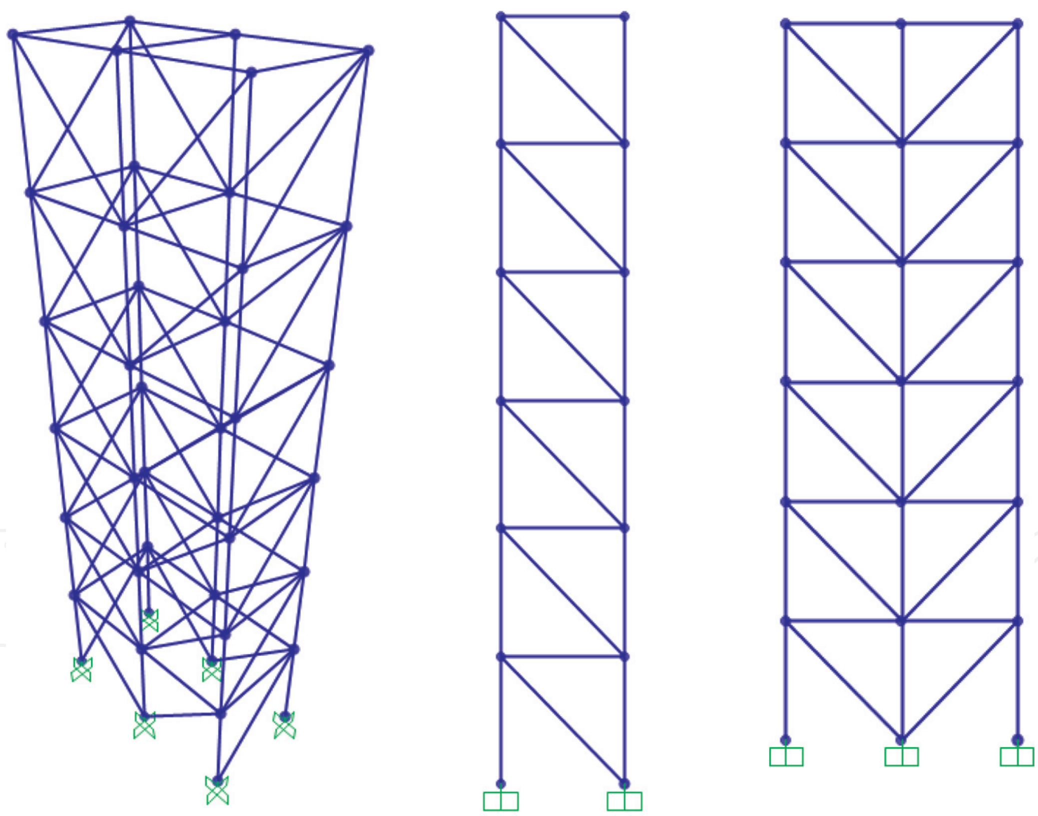

Figure 16.
One hundred fourteen members 3D frame—long and short façade.

$$\frac{\delta_{\max}(\mathbf{x})}{45} - 1 \leq 0$$
$$1 - \frac{f_1(\mathbf{x})}{4} \leq 0 \tag{18}$$

For this improved structure, the members are linked in five different groups described in **Table 11** and in **Figure 17**.

Group	Characteristics	Color
1	Corner columns	Red
2	Middle columns	Gray
3	Inner beams	Black
4	Outer beams	Blue
5	Bracers	Cyan

Table 11.
Experiment 4—members linked in five groups.

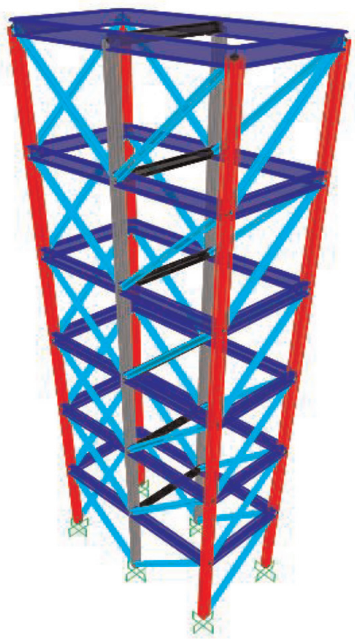

Figure 17.
Experiment 4—members linked in five groups according to **Table 11**.

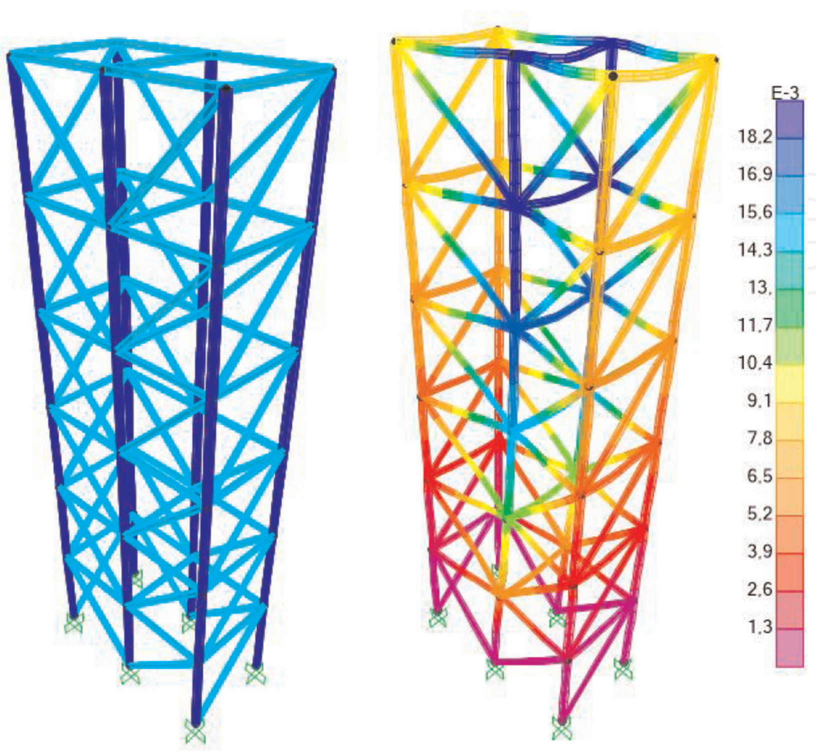

Figure 18.
The best solution and displacement field of Experiment 4.

Group	Characteristics	Color	Cross section
1	Corner columns	Blue	W 150 × 22.5
2	Middle columns	Blue	W 150 × 22.5
3	Inner beams	Cyan	W 150 × 13
4	Outer beams	Cyan	W 150 × 13
5	Bracers	Cyan	W 150 × 13
Maximum displacement		—	19 mm
First natural frequency		—	4.38 Hz
Total weight		—	6091 kg

Table 12.
The best solution of Experiment 4.

The best result found presented the lightest structure of this set of experiments, even though presenting a greater number of members than the previous structural configuration. The maximum displacement at the top of the frame is 19 mm, and the first natural frequency of vibration is 4.38 Hz, leading to a feasible solution. **Figure 18** and **Table 12** detail the best solution for this experiment.

5. Analysis of results

Two numerical experiments discussed concerning a three-storey 3D frame, in which it was possible to observe the importance of the natural frequency of vibration considered as a constraint. In general, it is neglected in the great majority of the structural optimization problems. The best solution found for Experiment 2 was heavier than the best solution found in Experiment 1. It can be justified since the first natural frequency of vibration was included in the problem formulation resulting in a heavier optimized structure.

A set of three experiments concerning a six-storey 3D frame were conducted with the members linked in three different groups. The constraints for these experiments are the maximum displacement at the top of the frame. The members were linked in two, four, and eight groups, and, as expected, the weights decrease as the number of linked bars increases. It is important to note from the results of the case where the members were linked in eight groups (Experiment 3.3) that the algorithm found only five distinct profiles.

Table 13 summarizes the results of Experiment 3, and the graphic in **Figure 19** is a curve of the tradeoff presenting a comparison of each one of the best solutions and their corresponding number of distinct profiles used.

Another important point was the fact that no feasible solutions were found for the six-storey frame with no bracings, considering the constraint concerning the first natural frequency of vibration. This fact indicated the conception of a new model increasing the stiffness of the structure to make possible a feasible optimized solution. Thus, bracings were considered in the new model increasing the total number of members. The result of Experiment 4 was very interesting leading to a lighter structure than the three other experiments (3.1, 3.2, and 3.3), even if presenting a more complex geometry with more members after the inclusion of the bracings in the model. The importance of the bracings in 3D steel frames was shown not only concerning their stability and stiffness but also improving its dynamic behavior.

Number of groups	Maximum displacement (mm)	Weight (kg)
2	22.6	8971
4	23	7851
8	26	7421

Table 13.
Analysis of results of Experiment 3.

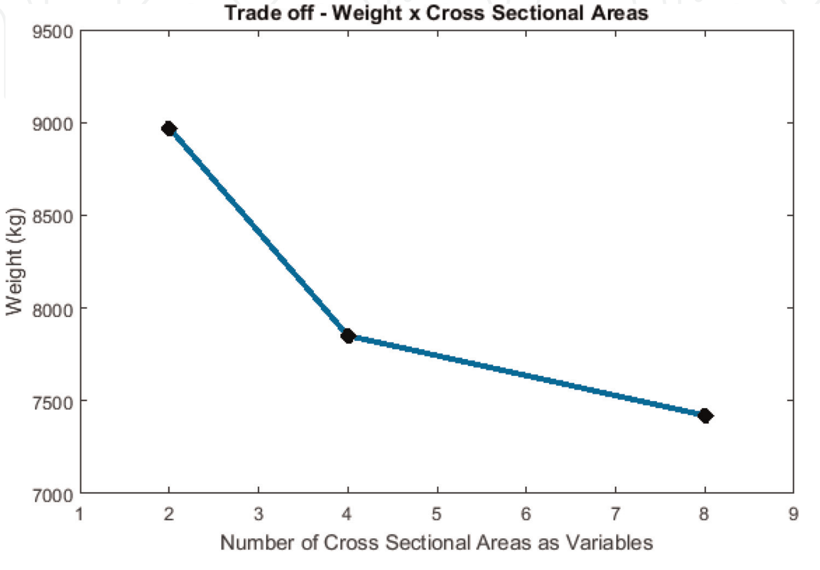

Figure 19.
Tradeoff curve of Experiment 3.

6. Conclusions and extensions

The study conducted in this chapter focused on the minimization of the weight of 3D steel frames, subjected to constraints concerning horizontal displacements and natural frequencies of vibration. It is interesting to note the importance of a structural optimization study before the design is conceived, which leads to more competitive and sometimes counterintuitive.

In the experiments addressed in this chapter, it is easy to conclude that the natural frequency of vibration is an essential characteristic to be considered in the formulation of the structural optimization problems.

As future works the approaches will extend to multi-objective optimization problems with more constraints, such as, stress, stability, geometry, and inter-storey drifts, introducing more real aspects to the optimization problems in engineering. Strategies should be considered for automatic grouping of members without the need for preliminary analysis by the designer. For this, special encodings will be used via cardinality constraints as can be seen in the structural optimization problems discussed in the references [20, 24, 25].

7. Remark

The codes used to solve the optimization problems presented in this chapter are written in Matlab® language, and the final results, as well as the figures, are checked by the SAP 2000®.

Acknowledgements

The authors wish to thank the reviewers that helped the quality of the chapter, Conselho Nacional de Desenvolvimento Científico e Tecnológico, CNPq (grant 306186/2017-9), and Fundação de Amparo à Pesquisa do Estado de Minas Gerais, FAPEMIG.

Conflict of interest

The authors declare that they have no conflicts of interest.

Author details

Cláudio H.B. Resende, José P.G. Carvalho, Afonso C.C. Lemonge*
and Patricia H. Hallak
Graduate Program in Civil Engineering, Federal University of Juiz de Fora,
Juiz de Fora, Brazil

*Address all correspondence to: afonso.lemonge@ufjf.edu.br

References

[1] AISC-ASD. Manual of Steel Construction-Allowable Stress Design. 9th ed. Chicago, IL, USA: American Institute of Steel Construction; 1989

[2] NBR 6123. Forces due to the wind in buildings. Brazilian Association of Technical Standards; Rio de Janeiro; 1988. (In Portuguese)

[3] NBR 8800. Design of steel structures and mixed structures of steel and concrete of buildings. Brazilian Association of Technical Standards; Rio de Janeiro; 2008. (In Portuguese)

[4] Artar M, Daloğlu AT. Optimum weight design of steel space frames with semi-rigid connections using harmony search and genetic algorithms. Neural Computing and Applications. 2018; **29**(11):1089-1100

[5] Maheri MR, Talezadeh M. An enhanced imperialist competitive algorithm for optimum design of skeletal structures. Swarm and Evolutionary Computation. 2018;**40**: 24-36

[6] Aydoğdu İ, Akın A, Saka MP. Design optimization of real world steel space frames using artificial bee colony algorithm with levy flight distribution. Advances in Engineering Software. 2016;**92**:1-14

[7] Talatahari S, Gandomi AH, Yang XS, Deb S. Optimum design of frame structures using the eagle strategy with differential evolution. Engineering Structures. 2015;**91**:16-25

[8] Maheri MR, Shokrian H, Narimani MM. An enhanced honey bee mating optimization algorithm for design of side sway steel frames. Advances in Engineering Software. 2017;**109**:62-72

[9] Kaveh A, BolandGerami A. Optimal design of large-scale space steel frames using cascade enhanced colliding body optimization. Structural and Multidisciplinary Optimization. 2017; **55**(1):237-256

[10] Jalili S, Hosseinzadeh Y, Taghizadieh N. A biogeography-based optimization for optimum discrete design of skeletal structures. Engineering Optimization. 2016;**48**(9): 1491-1514

[11] Gholizadeh S, Poorhoseini H. Optimum design of steel frame structures by a modified dolphin echolocation algorithm. Structural Engineering and Mechanics. 2015;**55**(3): 535-554

[12] Gholizadeh S, Milany A. An improved fireworks algorithm for discrete sizing optimization of steel skeletal structures. Engineering Optimization. 2018;**50**(11):1829-1849

[13] Hasançebi O. Cost efficiency analyses of steel frameworks for economical design of multi-storey buildings. Journal of Constructional Steel Research. 2017;**128**:380-396

[14] Memari AM, Madhkan M. Optimal design of steel frames subject to gravity and seismic codes' prescribed lateral forces. Structural Optimization. 1999;**18**: 56-66

[15] Kameshki ES, Saka MP. Genetic algorithm based optimum bracing design of nonswaying tall plane frames. Journal of Constructional Steel Research. 2001;**57**:1081-1097

[16] Liang QQ, Xie YM, Steven GP. Optimal topology design of bracing systems for multi-storey steel frames. Journal of Structural Engineering. 2000; **126**(7):823-829

[17] Pavlovčič L, Krajnc A, Beg D. Cost function analysis in the structural

optimization of steel frames. Structural and Multidisciplinary Optimization. 2004;**28**(4):286-295

[18] Storn R, Price K. Differential evolution a simple and efficient adaptive scheme for global optimization over continuous spaces. Technical Report; Berkeley, CA: University of California; 1995. 95-012

[19] Lemonge ACL, Barbosa HJC. An adaptive penalty scheme for genetic algorithms in structural optimization. International Journal for Numerical Methods in Engineering. 2004;**59**(5): 703-736

[20] Carvalho JP, Lemonge AC, Carvalho ÉC, Hallak PH, Bernardino HS. Truss optimization with multiple frequency constraints and automatic member grouping. Structural and Multidisciplinary Optimization. 2018;**57**(2):547-577

[21] Haftka RT, Kamat MP. Elements of Structural Optimization. Dordrecht: Martinus Nighoff; 1985

[22] Kaveh A, Javadi S. Shape and size optimization of trusses with multiple frequency constraints using harmony search and ray optimizer for enhancing the particle swarm optimization algorithm. Acta Mechanica. 2014; **225**(6):1595-1605

[23] Bathe KJ. Finite Element Procedures. Watertown, MA, USA: Prentice Hall, Pearson Education Inc.; 2006

[24] Barbosa HJ, Lemonge AC, Borges CC. A genetic algorithm encoding for cardinality constraints and automatic variable linking in structural optimization. Engineering Structures. 2008;**30**(12):3708-3723

[25] Lemonge AC, Barbosa HJ, Coutinho AL, Borges CC. Multiple cardinality constraints and automatic member grouping in the optimal design of steel framed structures. Engineering Structures. 2011;**33**(2):433-444